

SIZE DEPENDENCE ON MELTING OF COPPER NANOPARTICLES VIA MOLECULAR DYNAMICS SIMULATION

Cem Canan^{1*}, Murat Çeltek²

¹Edirne Vocational College of Technical Science, Trakya University, 22030, Edirne – Türkiye ²Faculty of Education, Trakya University, 22030, Edirne – Türkiye *Corresponding author: cemcanan@trakya.edu.tr

Abstract

In the last decay, increasing use of metallic nanoparticles (NPs) in nanotechnology have received great attention. Due to their strong surface and size effects, copper (Cu) NPs exhibits physical and more stable chemical properties such as thermal and electrical conductivity, mechanical strength compared to bulk Cu. Physical and chemical behavior of Cu NPs is important in design of nanoscale materials and devices. In this study, the melting behavior of Cu nanoparticles was investigated using classical molecular dynamics (MD) simulations. The atomic interactions were described by the embedded atom method (EAM) potential. We calculated the potential energy, pair distribution function, and diffusion coefficient of the systems to examine the size, temperature and melting process. From the simulation results, the melting temperature of Cu NPs decreases with decreasing particle size. However, the structural and dynamic properties are also dependent on particle size and temperature.

Keywords: Copper, Nanoparticle, Melting, Molecular Dynamics, Embedded Atom Method.

INTRODUCTION

Metallic nanostructures synthesized by different processes are used in fields such as electronics [1], [2], optoelectronics [3], and biosensors [4] due to their unique physical, chemical and electronic properties that distinguish them from the corresponding bulk materials. The main reason for the superior physical and chemical properties of nanostructures compared to bulk materials is their high surface-to-volume ratio [5]. During phase transition, nanostructures of thermodynamic properties also differ from bulk materials due to size effects [6]. The small size of NPs reduce the melting temperature and affect the chemical activity [7]. In the past decades because of their unusual properties and potential applications in many fields, considerable attention has been paid to Cu metal nanoparticles (NPs) [8]. Both experimental [9], [10] and theoretical studies [11],[12] have investigated the structures and properties of Cu NPs. Early MD simulations studies by Valkealahti and Manninen [13] and Garcia-Rodeja et al. [14] analyzed the dependence of melting temperature on cluster size. Dove and Wales [15] used Sutton-Chen potentials with Monte Carlo minimization to determine global minimum structures. Erkoç [16] investigated room-temperature structures of CuN clusters and the effects of radiation damage using empirical potentials and MD simulations. Grigoryan et al. [17] applied the embedded-atom method for detailed structural characterization of nanoclusters. The MD method employing the Quantum Sutton-Chen (Q-SC) manybody potential has been applied by Kart et al. [18] investigate the solid, liquid, and melting properties of Cu NPs. In this study, structural and dynamic properties of metallic Cu NPs such as potential energy, pair distribution function (PDF), and diffusion coefficients were investigated during the melting process using MD simulation with EAM force field.

EXPOSITION

Classical MD simulations were carried out using the DL_POLY [19] simulation package. Interatomic interactions among copper atoms were described using EAM potentials [20]:

$$E_T = \sum_{i=1}^N \left[\frac{1}{2} \sum_{i \neq j}^N \emptyset(r_{ij}) + F_i(\rho_i) \right]$$
 (1)

 $\emptyset(r_{ii})$ donates where the pairwise interaction potential energy function between atoms i and j, where as $F_i(\rho_i)$ represents the embedding energy, defined as the energy required to insert atom i into a site characterized by an electronic charge density ρ_i . The local electron density ρ_i is computed as the superposition of the individual atomic charge density contributions from all neighboring atoms surrounding atom i. The variable r_{ij} corresponds to the interatomic distance between atoms i and j. The EAM potential data from Sheng [21] were applied to characterize the interactions between Cu atoms. Both bulk Cu and spherical Cu NPs with diameters of 2.5 nm (NP-1), 5.0 nm (NP-2), 7.5 nm (NP-3), and 10.0 nm (NP-4) were studied. The bulk system consisted of 4000 atoms arranged in a face-centered cubic lattice, while NP-1, NP-2, NP-3 and NP-4 contained 675, 5473, 18749, and 44403 atoms, respectively. All spherical NPs were prepared by applying the cutting process from the ideal face-centered (fcc) crystal structure. The bulk Cu system was under the simulated NPT ensemble. maintaining constant temperature pressure with periodic boundary conditions applied in all three directions, whereas the NPs were simulated under the NVT ensemble constant volume and temperature without periodic boundary conditions, to mimic isolated clusters. The of classical equations motion using Leapfrog-Verlet integrated the algorithm with a time step of 1 fs. Temperature was controlled using the Nose-Hoover thermostat [22], and bulk pressure was maintained using the Berendsen barostat [23]. To obtain stable structures at 0 K, the initial configurations were first annealed at 300 K for 100000 MD steps and then cooled to 0 K at a rate of 0.05 K/ps. After annealing, the NPs remained nearly identical to their initial configuration, with only minor relaxation of surface atoms. For both bulk and NPs systems, the heating protocol involved a series of MD simulations in which the temperature was increased in increments of 100 K, while near the melting point the increment was reduced to 10 K to account for large temperature fluctuations. Each simulation was performed for 100000 MD steps, with the first 50000 steps used for equilibration and the remaining 50000 steps used to calculate time-averaged properties.

In the results section, we begin by examining the thermal properties commonly used to identify first-order phase transitions. It is well known that the melting temperature of a system can be estimated from the characteristic features of its caloric curve as a function of temperature. Figure 1 presents the temperature-dependent variations of the potential energy for both Cu NPs and the bulk system.

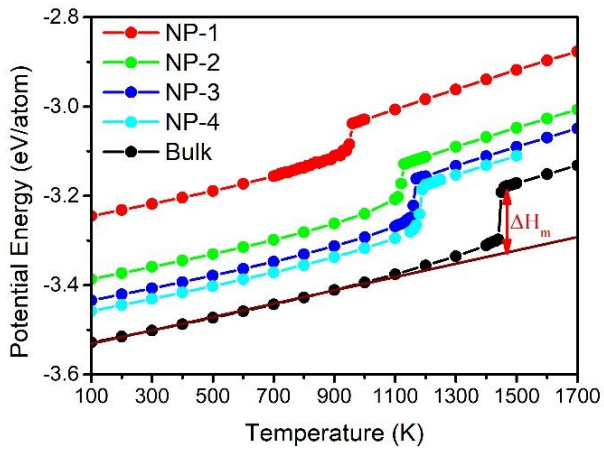


Fig. 1. Temperature dependence of potential energy for Cu NPs and bulk system.

The potential energy of the NPs and the bulk increases linearly with temperature at first. However, this linear trend is disrupted beyond a certain temperature, where a sharp rise in potential energy occurs. The temperature corresponding to this abrupt change is defined as the melting point, indicating the first-order phase transition. Above the melting temperature, the linear correlation between potential energy and

temperature resumes. Because of their higher surface energy, the potential energies of the NPs are greater than those of the bulk system. Moreover, the potential energy increases as the particle size decreases. Several thermodynamic quantities obtained from MD simulations including the melting temperature (T_m) , heat of fusion (ΔH_m) , lattice constant (a_o) , and cohesive energy (E_{coh}) are summarized in Table 1 for bulk system, along with available experimental data for comparison. The physical properties predicted for bulk Cu from MD simulations agree well with the experimental results.

Table 1. Physical properties of bulk Cu

	MD	Experimental
a, (Å)	3.61	3.61a
Ecoh(eV)	3.54	3.49a
$T_m(\mathbf{K})$	1440	1358ª
$\Delta H_m(Kj/mol)$	16.15	20.40 ^b

^a Ref.[24], ^b Ref. [25]

The variation of T_m and ΔH_m , estimated from calorific curves for Cu NPs, with particle size is shown in Figure 2. The T_m values of the NPs have significantly lower melting points compared to bulk Cu. Furthermore, this decrease in melting temperature becomes more pronounced as particle size decreases, confirming the strong influence of size effects on thermal stability. ΔH_m was calculated from the energy difference between the solid and liquid phases, as shown in Figure 1. The variation of ΔH_m with particle size follows a similar trend as T_m .

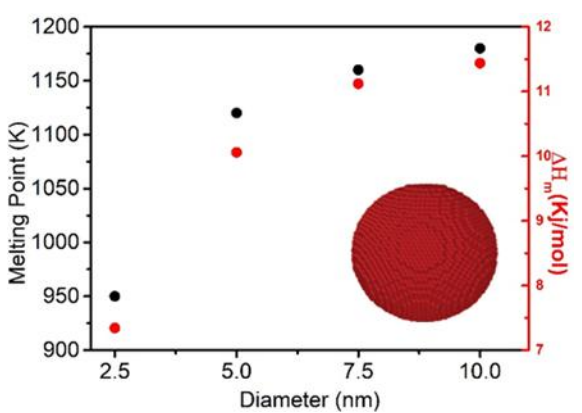


Fig. 2. Dependence of melting point and heat of fusion on particle size.

More specifically, smaller particles require less energy to achieve the solid-liquid phase transition, further strengthening the relationship between particle size and melting behavior.

The PDF represents the probability of finding a neighboring particle at a distance rfrom a selected reference atom or particle. Its form depends strongly on the state of matter and leads to significant differences among solids, amorphous materials, liquids, and gases. Due to this sensitivity to structural order, the PDF is considered one important of the most tools characterizing atomic arrangements. Therefore, it is widely used to study the structural properties of solid and liquid systems. The expression for g(r) of the PDF is as follows [26], [27]:

$$g(r) = \frac{\Omega}{N^2} \langle \sum_{i}^{N} \sum_{i \neq j}^{N} \delta(r - r_{ij}) \rangle$$
 (2)

To assess whether the EAM potential used to model interatomic interactions in MD simulations remains valid at temperatures, the PDF of liquid bulk Cu obtained from simulations is compared with available experimental measurements in Figure 3 [16]. As shown in Figure 3, the PDFs obtained from both MD simulations and experimental measurements exhibit the characteristic properties of the liquid phase. The agreement between the two results confirms the reliability of the simulation method we used.

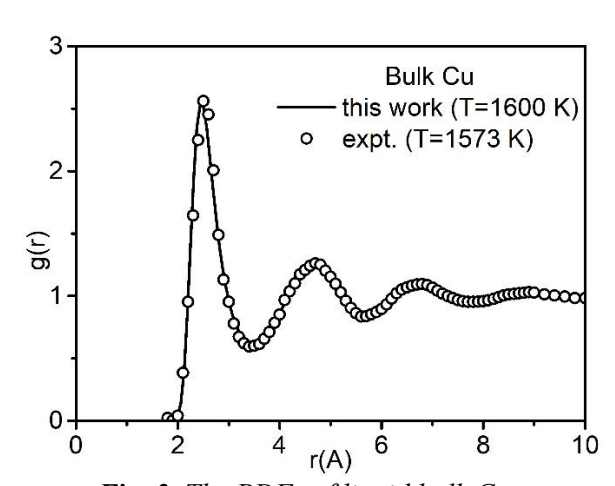


Fig. 3. The PDFs of liquid bulk Cu.

This consistency indicates that the EAM potential used in MD simulations is successful in reproducing the physical properties of bulk Cu, not only in the solid phase at low temperatures but also at high temperatures and in the liquid phase.

Figure 4 presents the PDFs of Cu NP-2 at various temperatures. At 300 K, the PDF shows the characteristic features of an ideal fcc crystal structure. As the temperature increases, the peaks are decrease while the peak widths broaden. The PDF at 1120 K characterizes both the crystalline and liquid phases. As expected, at the melting point a system displays both solid phase and liquid phase properties at the same time. Based on the PDF profiles of Cu NP-2, the melting temperature of the nanoparticle is identified as 1120 K.

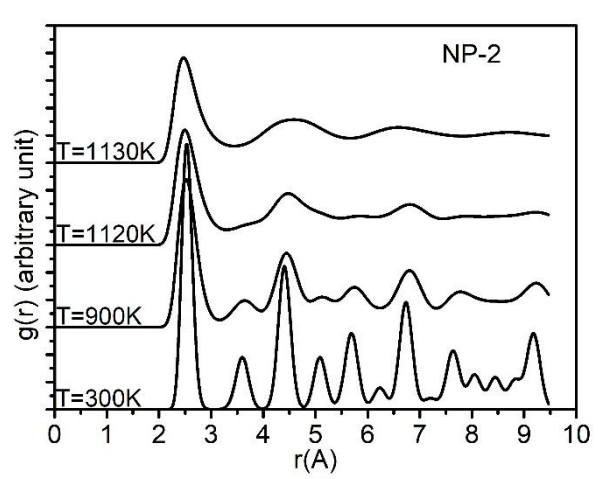


Fig. 4. PDFs of Cu NP-2 at different temperatures during the heating process.

This finding is consistent with the melting temperature found from the potential energy-temperature curve. At 1130 K, slightly above the melting temperature, PDF for NP-2 has completely lost its crystalline properties and shows typical properties. Also the melting behavior of a nanoparticle can be characterized by monitoring dynamic its properties, particularly the diffusion coefficients. The atomic diffusion coefficient, D, is defined by the Einstein equation, depending on the trajectories of the atoms within the NPs [26], [28]:

$$D = \lim_{t \to \infty} \frac{\frac{1}{N} \sum_{i=1}^{N} |r_i(t+t_0) - r_i(t_0)|^2}{6t}$$
 (3)

where t is the diffusion time, $r_i(t_0)$ is the position vector of the ith atom in its initial configuration for the system and $r_i(t)$ is the position vector of ith atom at time t.

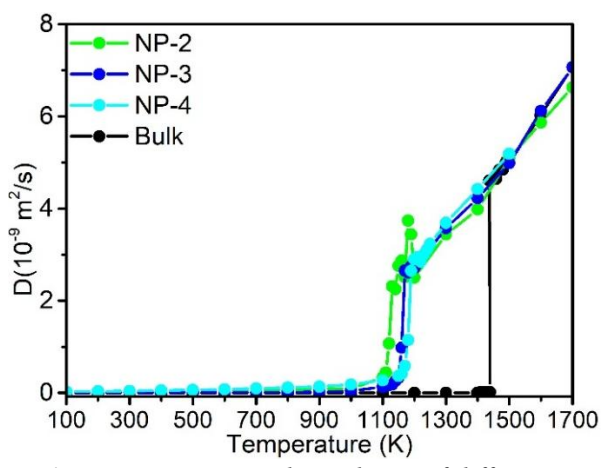


Fig. 5. Temperature dependence of diffusion coefficent for Cu NPs and bulk system.

Figure 5 displays the diffusion coefficients of Cu NPs and the bulk system as a function of temperature. A significant increase around the melting point was observed for all NPs and bulk Cu. This increase indicates that the atoms started to gain mobility and moved from solid-like behavior to liquid like behavior. Hence, the melting temperatures previously determined from thermal analyses are further confirmed by the dynamic response of the systems. At values above the melting point, the NP-2 diffusion coefficient is high and fluctuates more. However, the diffusion coefficients of larger nanoparticles, NP-3 and NP-4, shows a linear increase, similar to bulk Cu. This is explained by the fact that the surface-tovolume ratio increases with decreasing particle size. As a result, atoms at or near the surface become weaker and more sensitive to temperature.

CONCLUSION

In this work, the dynamic behavior of Cu nanoparticles with various sizes were investigated over a range of temperatures using molecular dynamics simulations based on the EAM force field. The simulation showed good agreement with available experimental data. As expected, both the melting temperature and the heat of fusion were found to increase with particle size, yet remained lower than those of the bulk material for all nanoparticle systems. The temperature evolution of the PDF was consistent with previous studies and bulk reference values. Dynamic analysis showed that rising temperature enhances the displacement of surface atoms from their lattice positions, leading to fluctuations in the diffusion coefficients above the melting point for smaller nanoparticles—an indication of surface diffusion or surface pre-melting.

Funding: No funding support has been received from any institution or person.

Acknowledgments: We would like to thank Trakya University Rectorate for giving permission and contributing to present this study as a paper.

REFERENCE

- [1] C. Wang, Y. Hu, C. M. Lieber, and S. Sun, Ultrathin Au Nanowires and Their Transport Properties, *J Am Chem Soc*, vol. 130, no. 28, Jul. 2008, pp. 8902–8903.
- [2] D. S. Hecht, L. Hu, and G. Irvin, Emerging Transparent Electrodes Based on Thin Films of Carbon Nanotubes, Graphene, and Metallic Nanostructures, *Advanced Materials*, vol. 23, no. 13, Apr. 2011, pp. 1482–1513.
- [3] N. C. Lindquist, P. Nagpal, K. M. McPeak, D. J. Norris, and S.-H. Oh, Engineering metallic nanostructures for plasmonics and nanophotonics, *Reports on Progress in Physics*, vol. 75, no. 3, Mar. 2012, p. 036501.
- [4] K. M. Byun, S. J. Yoon, D. Kim, and S. J. Kim, Experimental study of sensitivity enhancement in surface plasmon resonance biosensors by use of periodic metallic nanowires, *Opt Lett*, vol. 32, no. 13, Jul. 2007, p. 1902.
- [5] R. L. Johnston, *Atomic and Molecular Clusters*. CRC Press, 2002.

- [6] Y. Shibuta and T. Suzuki, A molecular dynamics study of the phase transition in bcc metal nanoparticles, *J Chem Phys*, vol. 129, no. 14, Oct. 2008.
- [7] A. V. Fedorov, A. V. Shulgin, and S. A. Lavruk, Description of melting of aluminum nanoparticles, *Combust Explos Shock Waves*, vol. 52, no. 4, Jul. 2016, pp. 457–462.
- [8] M. B. Gawande *et al.*, ChemInform Abstract: Cu and Cu-Based Nanoparticles: Synthesis and Applications in Catalysis, *ChemInform*, vol. 47, no. 19, Apr. 2016.
- [9] S. Chen and J. M. Sommers,
 Alkanethiolate-Protected Copper
 Nanoparticles: Spectroscopy,
 Electrochemistry, and Solid-State
 Morphological Evolution, *J Phys Chem B*, vol. 105, no. 37, Sep. 2001, pp. 8816–8820.
- [10] H. Häkkinen, M. Moseler, O. Kostko, N. Morgner, M. A. Hoffmann, and B. v. Issendorff, Symmetry and Electronic Structure of Noble-Metal Nanoparticles and the Role of Relativity, *Phys Rev Lett*, vol. 93, no. 9, Aug. 2004, p. 093401.
- [11] C. Massobrio, A. Pasquarello, and A. Dal Corso, Structural and electronic properties of small Cun clusters using generalized-gradient approximations within density functional theory, *J Chem Phys*, vol. 109, no. 16, Oct. 1998, pp. 6626–6630.
- [12] J. Oviedo and R. E. Palmer, Amorphous structures of Cu, Ag, and Au nanoclusters from first principles calculations, *J Chem Phys*, vol. 117, no. 21, Dec. 2002, pp. 9548–9551.
- [13] S. Valkealahti and M. Manninen, Structural transitions and melting of copper clusters, *Zeitschrift für Physik D Atoms, Molecules and Clusters*, vol. 26, no. 1, Mar. 1993, pp. 255–257.
- [14] J. García-Rodeja, C. Rey, L. J. Gallego, and J. A. Alonso, Molecular-dynamics study of the structures, binding energies, and melting of clusters of fcc transition and noble metals using the Voter and Chen version of the embedded-atom model, *Phys Rev B*, vol. 49, no. 12, Mar. 1994, pp. 8495–8498.
- [15] J. P. K. Doye and D. J. Wales, Global minima for transition metal clusters

- described by Sutton-Chen potentials, *New Journal of Chemistry*, vol. 22, no. 7, 1998, pp. 733–744.
- [16] Ş. Erkoç, Molecular-dynamics simulation of radiation damage on copper clusters, *International Journal of Modern Physics C*, vol. 11, no. 05, Jul. 2000, pp. 1025–1032.
- [17] V. G. Grigoryan, D. Alamanova, and M. Springborg, Structure and energetics of CuN clusters with (2≤N≤150): An embedded-atom-method study, *Phys Rev B*, vol. 73, no. 11, Mar. 2006, p. 115415.
- [18] H. H. Kart, H. Yildirim, S. Ozdemir Kart, and T. Çağin, Physical properties of Cu nanoparticles: A molecular dynamics study, *Mater Chem Phys*, vol. 147, no. 1–2, Sep. 2014, pp. 204–212.
- [19] W. Smith and T. R. Forester, DL_POLY_2.0: A general-purpose parallel molecular dynamics simulation package, *J Mol Graph*, vol. 14, no. 3, Jun. 1996, pp. 136–141.
- [20] U. Domekeli and M. Celtek, Structural and dynamic properties of aluminum nanoparticles during the melting process, *UNITECH – Selected Papers*, 2024.
- [21] H. Sheng, EAM potentials. Accessed: Oct. 16, 2025. [Online]. Available:

- https://sites.google.com/site/eampotentials/table/Cu
- [22] S. Nosé, A unified formulation of the constant temperature molecular dynamics methods, *J Chem Phys*, vol. 81, no. 1, Jul. 1984, pp. 511–519.
- [23] H. J. C. Berendsen, J. P. M. Postma, W. F. van Gunsteren, A. DiNola, and J. R. Haak, Molecular dynamics with coupling to an external bath, *J Chem Phys*, vol. 81, no. 8, Oct. 1984, pp. 3684–3690.
- [24] Charles. Kittel and Paul. McEuen, *Introduction to solid state physics*. Wiley, 2018.
- [25] https://www.webelements.com/copper/.
- [26] S. Dalgic and U. Domekeli, Melting properties of tin nanoparticles by molecular dynamics simulation, *J. Optoelectron. Adv. Mater.*, vol. 11, 2009, pp. 2126–2132.
- [27] U. Domekeli and M. Celtek, Melting mechanism of cylindrical molybdenum nanowire: A molecular dynamics simulation study, *UNITECH Selected Papers*, 2024.
- [28] Sengul S, Domekeli U, and Celtek M, Melting Behavior of Pb Nanowires: Molecular Dynamics Dimulations, in *International Scientific Conference UNITECH*, 2020, p. II-381.